STUDY OF THE INTERACTION OF CEFONICID SODIUM WITH BOVINE SERUM ALBUMIN BY FLUORESCENCE SPECTROSCOPY

Sh.-T. Duan, B.-Sh. Liu*, T.-T. Li, M.-M. Cui

College of Chemistry & Environmental Science, Hebei University, Baoding 071002, Hebei Province, China; e-mail: lbs@hbu.edu.cn

The reaction mechanism of cefonicid sodium with bovine serum albumin was investigated by traditional fluorescence spectroscopy and synchronous fluorescence spectroscopy. The results demonstrated that cefonicid sodium caused a strong fluorescence quenching of bovine serum albumin through a static quenching mechanism, during which the electrostatic force played the dominant role in this system, and the number of binding sites in the system was close to 1. It also showed that the primary binding site for cefonicid sodium was closer to tryptophan residues located in sub-hydrophobic domain IIA. Moreover, circular dichroism spectroscopy showed that the secondary structure of bovine serum albumin changed. The donor-to-acceptor distance $r < 8$ nm indicated that the static fluorescence quenching of bovine serum albumin was a non-radiation energy transfer process. The data obtained from $\Delta\lambda = 60$ nm and $\lambda_{ex} = 295$ nm indicated that synchronous fluorescence spectroscopy had higher sensitivity and accuracy compared to traditional fluorescence spectroscopy.

Keywords: *fluorescence quenching spectroscopy, synchronous fluorescence spectroscopy, UV-Vis absorption spectroscopy, circular dichroism spectroscopy, cefonicid sodium, bovine serum albumin.*

ИССЛЕДОВАНИЕ ВЗАИМОДЕЙСТВИЯ ЦЕФОНИЦИДА НАТРИЯ С БЫЧЬИМ СЫВОРОТОЧНЫМ АЛЬБУМИНОМ МЕТОДОМ ФЛУОРЕСЦЕНТНОЙ СПЕКТРОСКОПИИ

Sh.-T. Duan, B.-Sh. Liu*, T.-T. Li, M.-M. Cui

УДК 535.372:547.962.3

Колледж химии и экологии, Хэбэйский университет, Баодин 071002, провинция Хэбэй, Китай; e-mail: lbs@hbu.edu.cn

(Поступила 22 марта 2016)

С помощью традиционной, а также синхронной флуоресцентной спектроскопии исследован механизм взаимодействия цефоницида натрия с бычьим сывороточным альбумином (БСА). Показано, что цефоницид натрия вызывает сильное тушение флуоресценции БСА посредством статического механизма, при котором электростатическая сила играет доминирующую роль и число мест связывания в системе близко к единице. Основное место связывания для цефоницида натрия – вблизи остатков триптофана, расположенных в субгидрофобном домене IIA. Спектроскопия циркулярного дихроизма показывает, что вторичная структура БСА изменяется. Донорно-акцепторное расстояние $r < 8$ нм свидетельствует о том, что статическое тушение флуоресценции БСА представляет собой безызлучательный перенос энергии. Согласно результатам для $\Delta\lambda = 60$ нм и $\lambda_{ex} = 295$ нм, синхронная флуоресцентная спектроскопия обладает более высокой чувствительностью и точностью по сравнению с традиционной.

Ключевые слова: *спектроскопия тушения флуоресценции, синхронная флуоресцентная спектроскопия, абсорбционная спектроскопия ИК и видимого диапазона, спектроскопия циркулярного дихроизма, цефоницид натрия, бычий сывороточный альбумин.*

Introduction. Cefonicid sodium (CFS), with molecular weight of 586.53, is a second-generation broad spectrum, long-acting cephalosporin antibiotic. Its antibacterial activity is based on inhibiting the synthesis of bacterial cell walls. It is suitable for surgery infection prevention and the therapy of lower respiratory and urinary tract infections as well as the bacterial inflammation of skin, soft tissue, and joints.

Serum albumins are important soluble protein constituents of the circulatory system with multiple physiological functions. Bovine serum albumin (BSA) is a major component of bovine serum containing 607 amino acid residues. The study of the interaction between proteins and drugs has become one of the prime research topics in the fields of pharmacological, biological, and clinical medicine. Understanding the mechanism and related parameters of this interaction is crucial for understanding the pharmacodynamics and pharmacokinetics of drugs [1]. The main method employed for studying the interaction between proteins and small molecular ligands is spectroscopy, especially fluorescence spectroscopy. In traditional fluorescence spectroscopy, the binding mechanism between drug and protein is studied by examining the change of the protein fluorescence intensity at the maximum emission wavelength before and after adding the drug. In synchronous fluorescence spectrometry, excitation and emission monochromators are scanned simultaneously to study the reaction mechanism between protein and drug. Compared to traditional fluorescence spectroscopy, synchronous fluorescence spectrometry exhibits several advantages, such as good selectivity, high sensitivity, simplified spectra, narrowed bands, less interference [2], and simultaneous determination of the multicomponent mixture [3]. Synchronous fluorescence spectrometry is often used to study the conformational change of proteins and the polarity change around the chromophore microenvironment, but rarely used to study the binding mechanism. In this study, the binding mechanism of CFS and BSA was explored by traditional fluorescence quenching and synchronous fluorescence methods.

Experiment. The purity grade of CFS was inferior to 98.5%. BSA was purchased from Sigma-Aldrich (purity grade inferior 99%, Shanghai, China). Stock solutions of BSA (10.0 and 2.0 μM) and CFS (1.0 mM) were prepared. They were further diluted as working solutions before use. A Tris-HCl buffer solution containing NaCl (0.15 M) was used to keep the pH of the solution at 7.40, and a NaCl solution was used to maintain the ionic strength of the solution. All the reagents were of analytical grade, and all the aqueous solutions were prepared with fresh double-distilled water and stored at 277 K.

The UV-Vis experiment was carried out on a UV-Vis recording spectrophotometer (UV-265, Shimadzu, Japan) with 1.0 cm quartz cells; 1.0 mL of the Tris-HCl solution (pH 7.40), 2.0 mL of the BSA solution (10.0 μM), and CFS with different concentrations were added into a 10 mL colorimetric tube in succession. The samples were diluted to the mark with double-distilled water, mixed thoroughly by shaking, and kept static for 30 min at 298 K. The absorption spectra of BSA in the presence of CFS with different concentrations were recorded in the spectral range 190–350 nm.

All the fluorescence experiments were conducted on a Shimadzu RF-5301PC spectrofluorophotometer equipped with a CS501 superheated water bath (Nantong Science Instrument Factory). The experiments were carried out with a 1.0 cm path length cell. In a typical fluorescence measurement, 1.0 mL of the Tris-HCl solution (pH 7.40), 1.0 mL of the BSA solution (2.0 μM), and CFS were added into a 10 mL colorimetric tube in succession. The samples were diluted to the mark with double-distilled water, mixed thoroughly by shaking, and kept static for 30 min at different temperatures (298, 303, and 310 K). The excitation wavelengths for the BSA solution were 280 nm and 295 nm, respectively. The excitation and emission slits were set at 5 nm. The solution was subsequently scanned on the fluorophotometer, and the fluorescent intensity was determined at 340 nm.

Preparation of the solution for synchronous fluorescence measurement is described above. We recorded the synchronous fluorescence spectra of the BSA-CFS system when $\Delta\lambda$ values between the excitation and emission wavelengths were stabilized at 15 nm and 60 nm, respectively.

Circular dichroism (CD) measurements were performed on a MOS-450/SFM300 circular dichroism spectrometer (Bio-Logic, France) with a 1.0 mm path length quartz cuvette; 1.0 mL of the Tris-HCl solution (pH 7.40), 1.0 mL of the BSA solution (10.0 μM), and CFS were added into a 10 mL colorimetric tube in succession. The concentration ratio of protein and drug were 1:0, 1:10, and 1:20. The samples were diluted to the mark with water, mixed thoroughly by shaking, and kept static for 30 min at 298 K. Each spectrum was recorded at wavelengths between 200 nm and 300 nm with a scan speed of 1 nm/s.

Results and discussion. UV-Vis absorption measurements are a very simple method to explore the structural change and the complex formation [4]. It is well known that dynamic quenching would not cause a change in the UV spectrum of BSA. In contrast, static quenching would induce it [5]. When small molecules bind to BSA, its spectrum has two absorption peaks. The strong absorption peak at 210 nm reflects the

framework conformation of BSA and represents the absorption of BSA's characteristic polypeptide backbone structure C=O [6]. The weak absorption peak at 280 nm is due to the polarity of the microenvironment around the tyrosine and tryptophan residues of BSA [7]. The UV-Vis absorption spectra of BSA in the absence and presence of CFS are shown in Fig. 1. It can be seen that with the gradual addition of CFS to the BSA solution, the intensity of the peak at 210 nm decreased and an obvious red shift (210–215 nm) in the position of the absorbance peak was observed. This can be attributed to the interaction between CFS and BSA. This interaction resulted in the change of the peptide chain of BSA. The peak at 280 nm increased, and a blue shift in the spectra of the BSA-CFS system from 280 to 276 nm was observed, indicating that the microenvironment polarity of aromatic amino acid residues became larger [8]. Moreover, the experiment showed that the fluorescence quenching of BSA in our case was primarily caused by the CFS-BSA complex formation. This process is an example of static quenching.

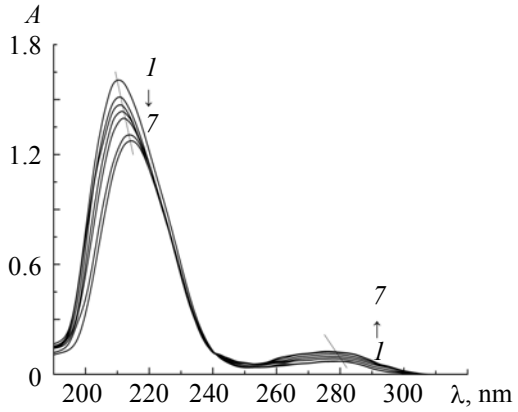

Fig. 1. Absorption spectra of the BSA-CFS system, T = 298 K, C_{BSA} = 2.0 μM, C_{CFS} = 0, 0.02, 0.05, 0.10, 0.15, 0.20, 0.25 mM.

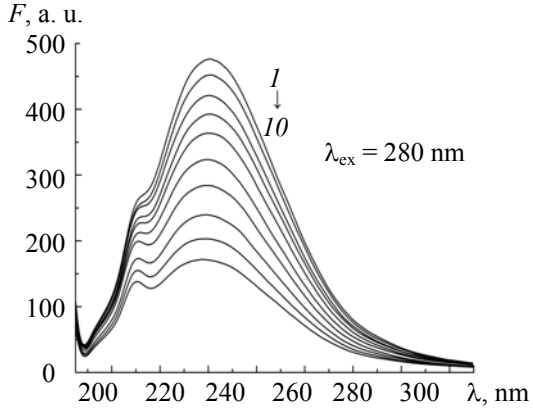

Fig. 2. Fluorescence spectra of the BSA-CFS system, T = 298 K, λ_{ex} = 280 nm, C_{BSA} = 0.20 μM, C_{CFS} = 0, 0.4, 2.0, 4.0, 8.0, 10.0, 20.0, 30.0, 40.0, 50.0 μM.

Proteins are considered to have intrinsic fluorescence due to the presence of amino acids, mainly tryptophan and tyrosine. The intrinsic fluorescence of protein is very sensitive to any change of the microenvironment [9]. When the excitation wavelength is fixed at 280 nm, tryptophan and tyrosine residues in BSA are excited, whereas at 295 nm, only tryptophan residues are excited [10]. Our experiments showed that, when the excitation wavelength was 280 nm (or 295 nm), BSA had a strong fluorescence emission peak at 340 nm. Fluorescence was not observed in CFS or the buffer solution in the experimental conditions. The fluorescence spectra of the BSA-CFS system (λ_{ex} = 280 nm) are shown in Fig. 2, demonstrating that the fluorescence intensity of BSA decreased regularly with the addition of CFS when the excitation wavelength was 280 nm (similar to 295 nm). This result showed that CFS could strongly quench the intrinsic fluorescence of BSA and that there was an interaction between CFS and BSA. Fluorescence quenching is usually classified

as dynamic or static. In static quenching, a new ground-state complex is generated between the fluorescent molecule and quencher. For its part, dynamic quenching is caused by the collision of the fluorescent molecule and quencher [11]. Different quenching mechanisms can be differentiated by their different dependences on temperature. At higher temperatures the diffusion and dissociation of weakly bound complexes occur faster. Therefore, the dynamic quenching constant increases with the increasing temperature whereas the static quenching constant decreases.

To determine the quenching mechanism, the fluorescence quenching data were analyzed using the Stern-Volmer Equation [12]:

$$F_0/F = 1 + K_q\tau_0[L] = 1 + K_{SV}[L], \quad (1)$$

where F_0 and F represent the fluorescence signals in the absence and presence of the quencher, respectively, τ_0 is the average lifetime of fluorescence without the quencher, which is about 10^{-8} s, K_{SV} is the Stern–Volmer quenching constant, K_q is the bimolecular quenching constant, and [L] is the concentration of the quencher. According to Eq. (1), based on the linear fit plot of F_0/F versus [L], the K_{SV} values can be obtained. The results are shown in Table 1. Table 1 demonstrates that the values of K_{SV} decreased with increase in temperature in all the systems, indicating that the probable quenching mechanism of the interaction between BSA and CFS was initiated by the complex formation rather than by the dynamic collision. In addition, all the values of K_q were much greater than the maximum scatter of the collision quenching constants of various quenchers (2.0×10^{10} L/mol/s), further suggesting that the reaction was a static process. It means that the system generated a new compound [13].

TABLE 1. Quenching Reactive Parameters of BSA and CFS

λ_{ex}, nm	T, K	K_q, L/mol/s	K_{SV}, L/mol	R_1	K_a, L/mol	n	R_2
280	298	4.55×10^{12}	4.55×10^{4}	0.9987	4.80×10^{4}	0.90	0.9991
	303	4.01×10^{12}	4.01×10^{4}	0.9986	4.19×10^{4}	0.91	0.9975
	310	3.80×10^{12}	3.80×10^{4}	0.9976	3.95×10^{4}	0.85	0.9970
295	298	2.44×10^{12}	2.44×10^{4}	0.9944	2.73×10^{4}	0.84	0.9989
	303	2.00×10^{12}	2.00×10^{4}	0.9985	2.05×10^{4}	0.81	0.9985
	310	1.93×10^{12}	1.93×10^{4}	0.9942	1.97×10^{4}	0.94	0.9975

N o t e. R_1 is the coefficient of proportionality in the linear dependence $F_0/F \sim [L]$; R_2 is the coefficient of proportionality in the linear dependence $\log[(F_0 - F)/F] \sim \log[L]$.

For static quenching, the relationship between the fluorescence intensity and the quencher concentration can be described by the following equation:

$$\log(F_0/F - 1) = n\log K_a + n\log\{[L] - n(1 - F/F_0)[B_t]\}, \quad (2)$$

where K_a is the binding constant, n is the number of binging sites, and [B_t] is the total concentration of BSA. From Eq. (2), K_a and n can be obtained. The results are shown in Table 1. They demonstrate that all the values of n were approximately equal to 1 at different temperatures, implying that there was just one binding site for CFS in BSA. Meanwhile, the values of K_a were of the order of 10^4, which indicated that there was a strong interaction between the CFS and the BSA. The binding constants between CFS and BSA decreased increasing temperature, which indicated that high temperature reduced the binding affinity of BSA and CFS, and the CFS-BSA complex was generated. This means that the quenching here was a static process [14]. As shown in Table 1, the binding constants for λ_{ex} = 280 nm were greater than for the case of λ_{ex} = 295 nm (at the same temperature). This indicated that tyrosine and tryptophan residues were both involved in the interaction of BSA and CFS.

In the BSA sub-hydrophobic domain, IIA (containing both tryptophan and tyrosine) and IIIA (containing only tyrosine) are the major binding sites of small molecule ligands [15]. On the basis of the Stern-Volmer equation, the participation of tyrosine and tryptophan groups in the BSA-CFS system was assessed by comparing the fluorescence quenching of BSA excited at 280 and 295 nm, and then the specific binding site was determined. Figure 3 shows that in the presence of CFS, the quenching curves of BSA excited at 280 and 295 nm did not overlap, and that the BSA quenching curve at 280 nm was much greater than that at 295 nm. This phenomenon shows that tryptophan and tyrosine residues were essential in the CFS-BSA interaction. Therefore, it implies that the primary binding site for CFS was sub-hydrophobic domain IIA.

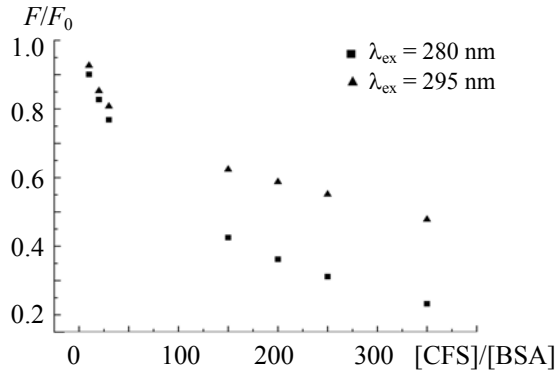

Fig. 3. Quenching curves of the BSA-CFS system, λ_{ex} = 280/295 nm, C_{BSA} = 0.20 μM, C_{CFS} = 2.0, 4.0, 6.0, 30.0, 40.0, 50.0, 70.0 Mm.

Synchronous fluorescence is an effective and simple tool to measure fluorescence quenching and the possible shift of the maximum emission wavelength [16]. When the Δλ value between the excitation and emission wavelengths is stabilized at 15 or 60 nm, the synchronous fluorescence gives characteristic information for tyrosine or tryptophan residues, respectively [17]. It can be seen from Fig. 4 that when Δλ = 15 nm, only a gradual fluorescence quenching was observed with the addition of CFS, while the maximum emission wavelength did not show a significant shift. The synchronous fluorescence spectra confirmed that tyrosine residues participated in the reaction, but the microenvironment around them did not undergo obvious changes during the binding process. However, when Δλ = 60 nm, a gradual decrease in the BSA fluorescence intensity and a red shift at the maximum emission wavelength were observed upon the addition of CFS, which indicated that a decrease in the hydrophobicity and an increase in the polarity surrounding tryptophan residue occurred. The results indicated that the BSA conformation was changed with the insertion of CFS [18]. Since tryptophan and tyrosine residues were both involved in the reaction, the synchronous fluorescence quenching ratios at Δλ = 15 and 60 nm were compared in order to further confirm the specific binding site of CFS to BSA. For comparison, the synchronous fluorescence quenching ratios (R_{SFQ}) that express the decreasing percentages of synchronous fluorescence intensity were calculated by using the equation $R_{SFQ} = 1 - F/F_0$ [19]. The corresponding ratios of synchronous fluorescence quenching (R_{SFQ}) are illustrated in Fig. 5. From Fig. 5 one can see that R_{SFQ} for Δλ = 60 nm was bigger than the corresponding one for Δλ = 15 nm, which revealed that the binding site of CFS to BSA was closer to tryptophan residues than to tyrosine ones.

In addition, synchronous fluorescence spectroscopy can be used to calculate the binding parameters. The results for Δλ = 60 and 15 nm, according to Eq. (1) and (2), are shown in Table 2. The obtained data can be used to estimate the quenching mechanism of the BSA-CFS system. From Table 2 one can see that the K_{SV} values decreased with increasing temperature in all systems, and the K_q values were much greater than

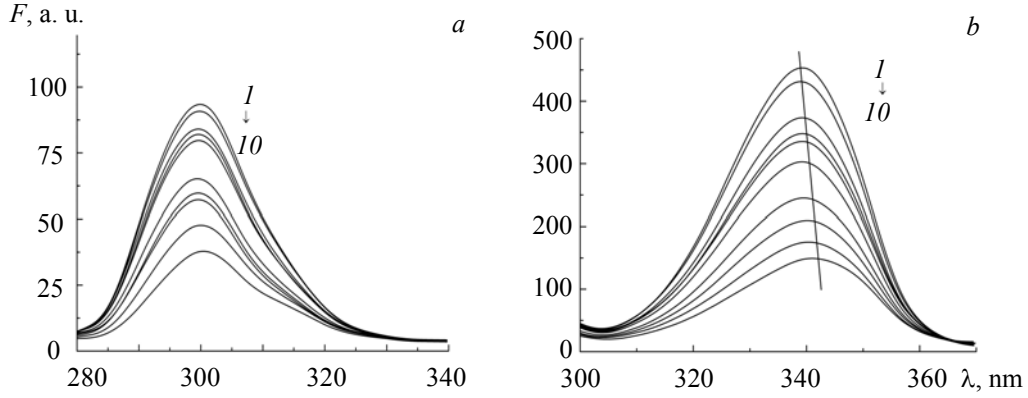

Fig. 4. Synchronous fluorescence spectra of the BSA-CFS system, T = 298 K, C_{BSA} = 0.20 μM, C_{CFS} = 0, 0.4, 2.0, 4.0, 8.0, 10, 20, 30, 40, 50 μM, Δλ = 15 (a) and 60 nm (b).

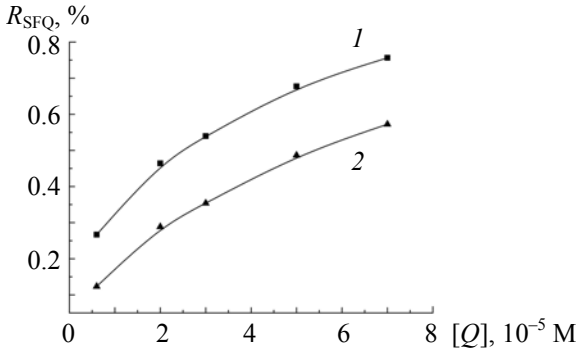

Fig. 5. Ratios of synchronous fluorescence quenching (R_{SFQ}) of the BSA-CFS system, T = 298 K, $\Delta\lambda$ = 60 (1) and 15 nm (2).

the maximum scatter collision quenching constant of various quenchers (2×10^{10} L/mol/s). This suggested that the quenching here was a static process that was initiated by the complex formation. The n values were close to 1, indicating that one molecule of CFS combines with one molecule of BSA. The K_a values were of the order of 10^4, and they decreased regularly with increasing temperature, which was coherent with the results obtained from the fluorescence quenching method. This indicated that the process was a static quenching. Comparing Table 1 and Table 2, the parameters obtained for $\Delta\lambda$ = 60 nm were greater than those for λ_{ex} = 295 nm. Therefore, the sensitivity in case of synchronous fluorescence is higher than in case of traditional fluorescence spectrometry, mainly due to the fact that synchronous fluorescence spectrometry has better selectivity. Thus, the synchronous fluorescence results are closer to the actual situation of the interaction between protein and small molecular ligands.

TABLE 2. Quenching Reactive Constant of CFS and BSA

$\Delta\lambda$, nm	T, K	K_{sv}, L/mol	K_q, L/mol/s	R_3	K_a, L/mol	n	R_4
15	293	2.01×10^4	2.01×10^{12}	0.9977	1.98×10^4	0.99	0.9962
	303	1.95×10^4	1.95×10^{12}	0.9991	1.81×10^4	0.78	0.9941
	310	1.75×10^4	1.75×10^{12}	0.9932	1.74×10^4	0.76	0.9932
60	293	4.21×10^4	4.21×10^{12}	0.9967	4.59×10^4	0.87	0.9980
	303	3.75×10^4	3.75×10^{12}	0.9972	4.05×10^4	0.94	0.9983
	310	3.51×10^4	3.51×10^{12}	0.9963	3.92×10^4	1.03	0.9968

N o t e. R_3 is the coefficient of proportionality in the linear dependence $F_0/F \sim [L]$; R_4 is the coefficient of proportionality in the linear dependence $\log [(F_0 - F)/F] \sim \log [L]$.

Generally, the nature of the interaction forces between the quencher and biomacromolecule can be obtained from the thermodynamic parameters. The thermodynamic parameters can be calculated on the basis of the Van't Hoff equation [20]:

$$\ln K_a = -\Delta H/RT + \Delta S/R, \quad (3)$$

$$\Delta G = \Delta H - T\Delta S = -RT\ln K_a, \quad (4)$$

$$\ln K_{a1}/K_{a2} = (\Delta H/R)(1/T_1 - 1/T_2), \quad (5)$$

where ΔH and ΔS are the standard variation of the enthalpy and entropy of the binding process, and R is the gas constant (R = 8.314 J/mol/K). According to Eqs. (3)–(5), values of K_a, ΔH, ΔS, and ΔG can be obtained at each temperature. They are listed in Table 3. The negative value of ΔG confirmed the spontaneous reaction between BSA and CFS. The negative value of ΔH and the positive value of ΔS show that CFS mainly bind to BSA by an electrostatic attraction [21]. The conclusions drawn from the synchronous fluorescence method were consistent with the traditional fluorescence quenching method. The values of ΔG calculated at $\Delta\lambda$ = 60 nm were smaller than those at λ_{ex} = 295 nm, indicating that the degree of spontaneous reaction was larger when $\Delta\lambda$ = 60 nm. This also showed that the synchronous fluorescence spectroscopy had higher sensitivity.

TABLE 3. Thermodynamic Parameter of the BSA-CFS System

T, K	K_a, L/mol	ΔH, kJ/mol	ΔS, J/mol/K	ΔG, kJ/mol
λ_{ex} = 280 nm				
298	4.80×10^4	–20.41	21.14	–26.71
303	4.19×10^4		21.12	–26.81
310	3.95×10^4		22.16	–27.28
λ_{ex} = 295 nm				
298	2.73×10^4	–20.88	14.86	–25.31
303	2.05×10^4		13.62	–25.01
310	1.97×10^4		14.86	–25.49
$\Delta\lambda$ = 15 nm				
298	1.98×10^4	–13.48	37.01	–24.51
303	1.81×10^4		37.03	–24.70
310	1.74×10^4		37.71	–25.17
$\Delta\lambda$ = 60 nm				
298	4.59×10^4	–18.79	26.17	–26.59
303	4.05×10^4		26.20	–26.73
310	3.92×10^4		27.32	–27.26

Fluorescence energy transfer can be separated into radiative and non-radiative energy transfer processes. According to Förster's non-radiative energy transfer theory, the concentrations of donor and acceptor are equal to the efficiency of energy transfer (E) and can be described by the following equations:

$$E = R_0^6/(R_0^6 + r^6) = 1 - F/F_0, \quad (6)$$

$$R_0^6 = 8.78\times10^{-25}K^2\Phi N^{-4}J, \quad (7)$$

$$J = \sum F(\lambda)\varepsilon(\lambda)\lambda^4\Delta\lambda/\sum F(\lambda)\Delta\lambda, \quad (8)$$

where E is the efficiency of energy transfer between the protein and ligand, r is the binding distance between the protein and ligand, R_0 is the distance for which the efficiency of the energy transfer is 50%, K^2 is the orientation factor in resonance energy transfer (assumed equal to 2/3), N is the refractive index of the medium (we suggest that N = 1.336), Φ is the fluorescence quantum yield of the donor in the absence of the acceptor (0.118 is used [22]), J is the overlap integral between the fluorescence emission spectrum of the donor and the absorption spectrum of the acceptor (Fig. 6), $F(\lambda)$ is the total fluorescence intensity of the fluorescence emission spectrum normalized to unity, $\varepsilon(\lambda)$ is the molar extinction coefficient of the acceptor (the CFS) at λ, and λ is the wavelength in cm. The J value can be calculated using Eq. (8), and E, R_0, and r can be calculated using Eqs. (6) and (7). The values are shown in Table 4. As can be seen from Table 4, the distance between BSA and CFS was less than 8 nm, which further indicated that the energy transfer from BSA to CFS occurred with high probability, and it was a non-radiative process [23]. The results obtained from the synchronous fluorescence method and the traditional fluorescence quenching method both prove that the BSA-CFS system is an example of non-radiative energy transfer, which verified the accuracy of the synchronous fluorescence spectroscopy method to judge the quenching mechanism.

CD is a sensitive technique to monitor any type of conformational change in proteins upon interaction with a drug molecule. The CD spectra of BSA at the pH 7.4 in the absence and presence of CFS are shown in Fig. 7. As evident from Fig. 7, the CD spectra of free BSA displayed two negative peaks at 208 and 222 nm, which was due to the α-helix structure of BSA [24] and the $n\rightarrow\pi^*$ transition for the peptide bond of the α-helix [25]. The BSA band intensities at 208 and 222 nm increased upon the addition of CFS, which indicated that there was an enhancement of the α-helical content of BSA after binding to CFS [26]. This showed that the secondary structure of BSA had been changed. But the CD spectra of BSA in the absence and presence of CFS were observed to be similar in shape, implying the structure of the protein was also predominantly α-helix even after binding to CFS [27].

TABLE 4. Parameters of E, J, R_0, r between BSA and CFS

T, K	E, %	J, cm^3· L/mol	R_0, nm	R, nm
Fluorescence quenching				
298	2.96	1.12×10^{-14}	2.50	4.47
303	2.48	1.14×10^{-14}	2.50	4.62
310	2.00	1.13×10^{-14}	2.50	4.78
Synchronous fluorescence				
298	2.97	1.11×10^{-14}	2.50	4.47
303	2.35	1.12×10^{-14}	2.50	4.65
310	1.71	1.12×10^{-14}	2.50	4.90

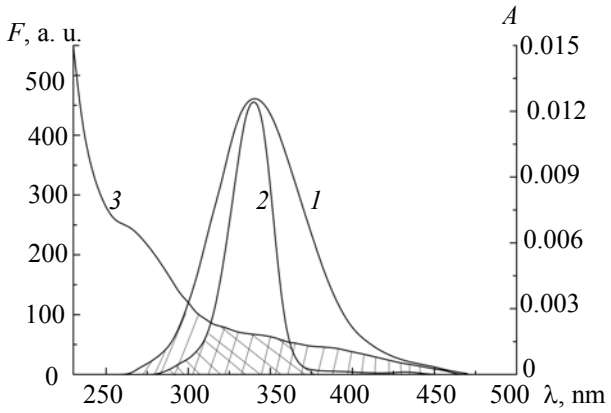

Fig. 6. Overlap of the fluorescence spectrum of BSA, λ_{ex} = 280 nm (1) and $\Delta\lambda$ = 60 nm (2) with the absorption spectrum of CFS (3), T = 298 K, $C_{CFS} = C_{BSA}$ = 0.20 μM.

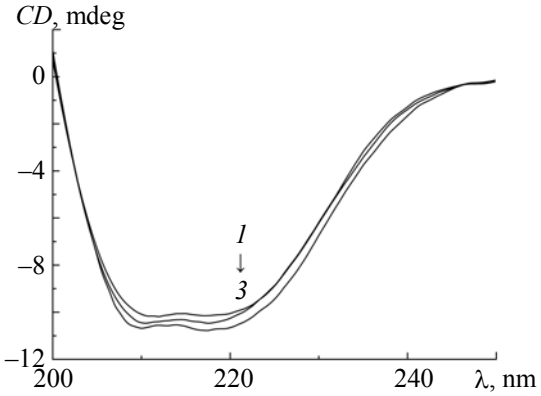

Fig. 7. Circular dichroism spectra of the BSA-CFS system (BSA (1), C_{BSA}:C_{CFS} = 1:10 (2) and 1:20 (3)), T = 293 K, C_{BSA} = 1.0 μM, C_{CFS} = 0, 10.0, 20.0 μM.

Conclusion. The interaction between CFS and BSA under simulated physiological conditions was investigated using fluorescence quenching and synchronous fluorescence spectroscopy. These two methods used the same equations to describe the processes and were based on the similar principles. However, by comparing the data obtained from $\Delta\lambda$ = 60 nm and λ_{ex} = 295 nm, which both represent tryptophan residues, we showed that the binding constants in the case of synchronous fluorescence spectrometry were greater than in the case of traditional fluorescence spectrometry. This is mainly due to the fact that synchronous fluorescence spectrometry has better selectivity, which in turn can help dodge different perturbing effects. Therefore, the method has higher sensitivity and the experimental data obtained from synchronous fluores-

cence spectrometry better describe the interaction between drug and protein. The values of ΔG were smaller at $\Delta\lambda$ = 60 nm than at λ_{ex} = 295 nm, which also indicated that synchronous fluorescence spectroscopy had higher sensitivity. Thus, synchronous fluorescence spectroscopy can be used to study the reaction mechanism between drug and protein.

Acknowledgment. The authors are grateful to the National Science Foundation of China (No. 21375032) for financial support.

REFERENCES

1. A. D. Bani-Yaseen, *J. Lumin.*, **131**, No. 5, 1042–1047 (2011).
2. X. R. Li, Y. B. Hao, *J. Mol. Struct.*, **1091**, 109–117 (2015).
3. Y. F. Wei, X. H. Li, D. M. Ma, *Spect. Anal.*, **25**, No. 4, 588–590 (2005).
4. H. M. Zhang, Y. Y. Wang, Q. H. Zhou, *J. Mol. Struct.*, **921**, 156–162 (2009).
5. Q. Wang, S. R. Zhang, X. H. Ji, *Spectrochim. Acta. A*, **124**, 84–90 (2014).
6. Y. P. Wang, G. W. Zhang, L. H. Wang, *Pestici. Biochem. Phys.*, **108**, 66–73 (2014).
7. L. Z. Zhao, Y. S. Zhao, H. H. Teng, S. Y. Shi, B. X. Ren, *J. Appl. Spectrosc.*, **81**, No. 4, 719–724 (2014).
8. L. Tang, S. Li, H. N. Bi, X. Gao, *Food Chem.*, **196**, 550–559 (2016).
9. H. B. Shen, Z. Q. Gu, K. Jian, *J. Pharm. Biomed.*, **75**, 86–93 (2013).
10 L. H. Zhang, B. S. Liu, Z. Y. Li, *Spectrosc. Let.*, **48**, 441–446 (2014).
11. S. Roy, T. K. Das, *J. Appl. Spectrosc.*, **82**, No. 4, 598–606 (2015).
12. Y. M. Yang, D. J. Li, C. Xu, *J. Mol. Struct.*, **1084**, 229–235 (2015).
13. T. H. Wang, Z. M. Zhao, L. Zhang, L. Ji, *J. Mol .Struct.*, **937**, No. 1-3, 65–69 (2009).
14. A. Naseri, S. Hosseini, F. Rasoulzadeh, *J. Lumin.*, **157**, 104–112 (2015).
15. A. Sułkowska, M. Maciążek-Jurczyk, B. Bojko, J. Rownicka, I. Zubik-Skupien, E. Temba, D. Pentak, W. W. Sulkowski, *J. Mol. Struct.*, **881**, No. 1-3, 97–106 (2008).
16. Z. X. Liao, X. Y. Yu, Q. Yao, P. G. Yi, *Spectrochim. Acta. A*, **129**, 314–319 (2014).
17. Y. Y. Hu, S. Q. Xu, X. S. Zhu, *Spectrochim. Acta. A*, **74**, No. 2, 526–531 (2009).
18. N. Ji, C. Qiu, X. J. Li, L. Xiong, Q. J. Sun, *Colloid Surf. B*, **128**, 594–599 (2015).
19. D. D. Chen, Q. Wu, J. Wang, Qi. Wang, H. Qiao, *Spectrochim. Acta. A*, **135**, 511–520 (2015).
20. A. Iovescu, A. Băran, G. Stîngă, *J. Photochem. Photobiol. B*, **1**, No. 4, 198–205 (2015).
21. Y. Fan, Y. Li, H. Cai, J. Li, J. Miao, D. Fu, Q. Yang, *J. Appl. Spectrosc.*, **81**, No. 5, 795–800 (2014).
22. H. X. Bai, C. Yang, X. R. Yang, *Front. Chem. China*, **3**, No. 1, 105–111 (2008).
23. N. Wang, L. Ye, F. F. Yan, R. Xu, *Int. J. Pharm.*, **351**, No. 1-2, 55–60 (2008).
24. G. Siligardi, R. Hussain, S. G. Patching, *BBA Biomembranes*, **1838**, 34–42 (2014).
25. S. Tabassum, W. M. Al-Asbahy, M. Afzal, F. Arjmand, *J. Photochem. Photobiol. B*, **114**, 132–139 (2012).
26. N. Keswani, N. Kishore, *J. Chem. Thermodyn.*, **43**, 1406–1413 (2011).
27. X.Y. Yu, B. F. Jiang, Z. X. Liao, Y. Jiao, P. G. Yi, *Spectrochim. Acta. A*, **149**, 116–121 (2015).